Inflammation, Vol. 42, No. 2, April 2019 (© 2018)
DOI: 10.1007/s10753-018-0921-5

ORIGINAL ARTICLE

MiR-590-3p Attenuates Acute Kidney Injury by Inhibiting Tumor Necrosis Factor Receptor-Associated Factor 6 in Septic Mice

Jing Ma,[1] Yu-tao Li,[1] Shi-xiong Zhang,[1] Shou-zhi Fu,[1,2] and Xian-zhi Ye[1,2]

Abstract— Previous studies have been indicated that tumor necrosis factor receptor-associated factor 6 (TRAF6)-induced inflammation leads to acute kidney injury (AKI). How microRNA (miR) contributes to this process is poorly defined. The aim of this study was to investigate whether miR-590-3p regulated lipopolysaccharide (LPS)-induced inflammatory response by inhibiting TRAF6. LPS-induced septic mice were treated with adenovirus expressing miR-590-3p (ad-miR-590-3p) *via* tail-vein injection. AKI was evaluated by examining serum cystatin C (CysC), serum β2-microglobulin (β2-MG), and blood urea nitrogen (BUN). The mRNA and protein levels were assayed by RT-qPCR and western blotting, respectively. The proliferation of podocytes was monitored using the MTT assay. Cell apoptosis was analyzed by flow cytometry. Survival outcomes in ad-miR-590-3p-transfected septic mice were markedly improved compared with mice with LPS-induced sepsis. Ad-miR-590-3p transfection significantly attenuated LPS-induced AKI, which was reflected by an improved glomerular filtration rate (GFR) as determined by measuring CysC, β2-MG, and BUN. Moreover, we observed that miR-590-3p was a novel regulator of TRAF6, binding to its 3′-untranslated regions (3′-UTRs). *In vitro*, a miR-590-3p gain-of-function mutation blocked LPS-induced podocyte growth inhibition and apoptosis, as well as overactivation of the inflammatory response. miR-590-3p has the ability to suppress LPS-induced AKI and podocyte apoptosis by targeting TRAF6. This might provide a novel strategy for the treatment of LPS-induced renal injuries.

KEY WORDS: miR-590-3p; sepsis; AKI; TRAF6; inflammatory response; apoptosis.

INTRODUCTION

Sepsis is one of the leading causes of death in intensive care units (ICUs) and is characterized by a severe bacterial infection, which can induce the occurrence of a systemic inflammatory response syndrome and can lead to multiple organ failure, including acute kidney injury (AKI) [32, 47]. Sepsis-induced AKI has been reported as an independent risk factor for death in septic patients, and in fact, greater than 50% of the mortality in ICUs is associated with sepsis-induced AKI [15, 23]. To improve the treatment of sepsis-induced AKI, a better understanding of its pathogenesis is required. A great deal of evidence suggests that sepsis-induced AKI involves the overactivation of pro-inflammatory mechanisms [34]. Several proinflammatory cytokines, including interleukin (IL)-1β, IL-6, tumor necrosis factor (TNF)-α, and monocyte

[1] Department of Emergency, Optics Valley hospital, Wuhan Third Hospital of Wuhan University, No. 216 Guanshan Road, Wuhan, 430073, China
[2] To whom correspondence should be addressed at Department of Emergency, Optics Valley hospital, Wuhan Third Hospital of Wuhan University, No. 216 Guanshan Road, Wuhan, 430073, China. E-mails: sz_futh@aliyun.com; xianzhi_ye123@163.com

chemoattractant protein-1 (MCP-1), have been implicated in the development of sepsis-induced AKI [48].

TRAF6 as an adaptor protein is a member of the TRAF family and mediates a wide array of protein-protein interactions *via* its TRAF domain as well as a RING finger domain that possess a nonconventional E3 ubiquitin ligase activity [35]. Recent studies have shown that excessive inflammatory responses mediated by TRAF6 triggers the production of inflammatory cytokines by activating nuclear transcription factor-kappa B (NF-κB) signaling [13, 25]. Usually, TRAF6 forms a homodimer and catalyzes K63-linked ubiquitination, which is essential for the activation of toll-like receptor 4 (TLR4)-dependent NF-κB signaling [7]. In contrast, K48-linked ubiquitination can promote TRAF6 degradation through the proteasome and block the inflammatory signal transduction in the TLR4 pathway [46]. Lipopolysaccharide (LPS) is a known ligand of TLR4 that can activate the inflammatory response by mediating the TRAF6/NF-κB pathway and upregulating the inflammatory cytokine levels [4, 10]. In LPS- and cecal ligation and puncture (CLP)-induced septic mice, TRAF6 protein expression is markedly upregulated in liver and heart tissues, respectively, while suppression of TRAF6 expression is accompanied by the inhibition of the extreme inflammatory status and tissue injuries [14, 17, 27]. These findings suggest that inactivation of TRAF6 signaling may be an efficient approach for inhibiting excessive inflammatory responses. However, the effects of posttranscriptional mechanisms on TRAF6 expression remains unclear.

MiRs as a class of noncoding single-stranded RNAs (18–25) have recently emerged as posttranscriptional regulators involved in a variety of biological processes *via* the regulation of gene expression through the binding to the 3′-UTRs of their target genes [41]. Recent studies have demonstrated that the TLR-mediated TRAF6/NF-κB signaling cascades can be targeted by miRs [5, 27]. In high glucose-treated human gingival fibroblasts, miR-126 regulates inflammatory cytokine secretion *via* the regulation of TRAF6 [39]. Moreover, a number of different miRs, including miR-144, miR-146a, and miR-146b-5p, have been found to regulate TRAF6 expression both *in vitro* and *in vivo* [19, 31, 33, 44]. miR-125b and miR-146a protect against sepsis-induced cardiac dysfunction by suppressing TRAF6 and NF-κB activation [9, 27]. In addition, miR-146a targeting to TRAF6 is involved in LPS-induced cross-tolerance against kidney injury [5]. These results reveal that TRAF6 can be targeted by multiple miRs in sepsis-induced tissue damage and inflammatory responses [1, 9, 24, 27].

MiR-590-3p is widely expressed in various tissues and cells, such as the human heart, endothelial progenitor cells and human mesenchymal stem cells [16, 18, 37]. MiR-590-3p regulates multiple signaling pathways, including salt overly sensitive 2 interaction protein 1, NF-κB, and angiotensin II, which are involved in epithelial-mesenchymal transition, myocarditis, and endothelial injury, respectively [38, 49, 51]. To the best of our knowledge, there have been no reports on miR-590-3p in LPS-induced AKI. In the present study, by utilizing online prediction algorithms, we have identified that TRAF6 is a direct target of miR-590-3p. The aim of our current study was to investigate whether adenovirus expressing miR-590-3p (ad-miR-590-3p) could attenuate LPS-induced AKI *in vivo* and podocyte apoptosis *in vitro* by inhibiting TRAF6 expression.

MATERIALS AND METHODS

Cell Culture

Mouse podocytes (MPC5) were purchased from the National Infrastructure of Cell Line Resource (Serial number: 3111C0001CCC000230; Beijing, China) and were incubated in Dulbecco's Modified Eagle's medium (DMEM; Thermo Fisher Scientific, Inc., Waltham, MA, USA) and supplemented with 10% FBS, 100 μg/mL streptomycin, and 100 IU/mL penicillin (all purchased from Sigma-Aldrich). All of the experiments were repeated with at least three different cell preparations in triplicate.

3-(4,5-Dimethyl-2-yl)-2,5-Diphenyltetrazolium Bromide (MTT)

Cell viability was monitored using the MTT assay (Beyotime Institute of Biotechnology, Haimen, China) as described previously [3]. The absorbance at 490 nm was obtained using a SpectraMax M5 ELISA plate reader (Molecular Devices, LLC, Sunnyvale, CA, USA).

Flow Cytometry for Apoptosis

Annexin V-FITC/PI apoptosis detection kit was purchased from Invitrogen (Carlsbad, Calif, USA). The cell apoptosis assay was performed by flow cytometry assay (FACScan, BD Biosciences, San Jose, CA, USA) and analyzed using CELL Quest 3.0 software (BD Biosciences).

Animal Treatment

The experiment was approved by the Ethics Committee of the Wuhan three hospital of Wuhan University (Wuhan, China) and performed in accordance with its guidelines. A total of 80 male 8-week-old C57BL/6J mice (body weight, 20 ± 2 g) were obtained from the Vital River Laboratory Animal Technology Co., Ltd. (Beijing, China) and allowed to acclimate to the environment for 1 week. The mice were given free access to food and tap water and were individually caged under controlled temperature (23 ± 2 °C) and humidity (55 ± 5%) with an artificial 12-h light/dark cycle. The mice were randomly divided into four groups as follows: the NC group was injected with normal saline; the LPS group was given 20 mg/kg of LPS intraperitoneally; the LPS (20 mg/kg) + ad-miR-Con group was transfected with adenovirus carrying scrambled hairpin; the LPS (20 mg/kg) + ad-miR-590-3p group was transfected with adenovirus carrying miR-590-3p (1×10^9 plaque-forming units) by tail-vein injection twice within 24 h. In another experiment, we observed the 96-h survival of CLP mice with or without ad-miR-590-3p (twice/day) treatment ($n = 10$ in each group).

Enzyme-Linked Immunosorbent Assay (ELISA)

The levels of inflammatory cytokines, tumor necrosis factor α (TNF-α; cat. no: E-EL-M0049c), interleukin-1β (IL-1β; cat. no: E-EL-M0037c), and interleukin 6 (IL-6; cat. no: E-EL-M0044c) were measured by mouse ELISA kit (Elabscience Biotechnology Co., Ltd., Wuhan, China) with a SpectraMax M5 ELISA plate reader (Molecular Devices, LLC, Sunnyvale, CA, USA) according to the manufacturer's instructions.

Measurement of Glomerular Filtration Rate (GFR)

Serum cystatin C (CysC) and β2-microglobulin (β2-MG) are freely filtered by the glomerular membrane, making blood levels of these compounds good indicators of GFR function. For this purpose, CysC (cat. no: CYS4004) and β2-MG (cat. no: RQ9114) were measured using the RANDOX enzymatic creatinine assay (Randox Laboratories Limited, Crumlin, Antrim, UK). Blood urea nitrogen (BUN) was measured *via* an enzymatic kinetic method using commercial kits (cat. no: C013-2; Nanjing Jiancheng Biology Engineering Institute, Nanjing, China).

Transfection with miR-590-3p Mimics and Inhibitors

The miR-590-3p mimic (5′-UAAUUUUAUGUAUAAGCUAGU-3′) and miR-590-3p-Con (5′-UCCGGGUGCCGCCGUAAGCUC-3′) sequences were synthesized by RiboBio (Guangzhou, China). The podocytes were transfected using Lipofectamine 2000 (Invitrogen; Thermo Fisher Scientific, Inc.) at a final concentration of 100 nM. At 48-h posttransfection, the cells were harvested for analysis.

Dual-Luciferase Reporter Gene Assay

The potential binding sites between miR-590-3p and TRAF6 were obtained using the online prediction software miRanda (www.microrna.org) and synthesized by RiboBio (Guangzhou, China). The wild-type (WT) and mutant-type (MUT) 3′-UTR of TRAF6 were inserted into the multiple cloning site of the luciferase expressing vector pMIR-REPORT (Ambion; Thermo Fisher Scientific, Inc.). For the luciferase assay, the podocytes (1×10^5) were seeded into 24-well plates and cotransfected with luciferase reporter vectors containing the WT and MUT of TRAF6-3′-UTR (0.5 μg) and mimics or control sequences of miR-590-3p (100 nM) using Lipofectamine 2000 (Invitrogen; Thermo Fisher Scientific, Inc.). The luciferase activity was measured using the Dual-Luciferase Reporter® Assay System (cat. no: E1960; Promega, USA) on a Luminoskan™ Ascent Microplate Luminometer (Thermo Fisher Scientific, Waltham, MA, USA).

Recombinant Adenoviruses

Recombinant adenoviruses for expression of miR-590-3p (ad-miR-590-3p) or control scrambled short hairpin RNA (ad-miR-Con) were generated using the BLOCK-iT adenoviral RNAi expression system (Invitrogen, Carlsbad, CA) according to the manufacturer's instructions. High-titer stocks of amplified recombinant adenoviruses were purified as described previously [40]. Viruses were diluted in PBS and administered at a dose of 10^7 plaque-forming units per well in 12-well plates, and 10^9 plaque-forming units per mouse *via* tail-vein injection.

Reverse Transcription-Quantitative Polymerase Chain Reaction (RT-qPCR)

Total RNA was extracted by TRIzol (Invitrogen) according to the manufacturer's protocol. The cDNA was synthesized by reverse transcription reactions with 2 μg of total RNA using Moloney murine leukemia virus reverse transcriptase (Invitrogen; Thermo Fisher Scientific, Inc.) according to the manufacturer's protocol. PCR reaction mixtures (20 μl) were prepared using TaqMan Universal PCR Master Mix (Thermo Fisher Scientific, Inc.)

and performed using a DNA Engine (ABI 7300; Thermo Fisher Scientific, Inc.). The reaction conditions were set according to the manufacturer's protocol. The Cq (quantification cycle fluorescence value) was calculated using SDS software, version 2.1 (Applied Biosystems; Thermo Fisher Scientific, Inc.), and the relative expression levels of miR and mRNA were calculated using the $2^{-\Delta\Delta Cq}$ method [22] and normalized to the internal control U6 and glyceraldehyde 3-phosphate dehydrogenase (GAPDH), respectively. The following primers were synthesized by Sangon Biotech (Shanghai, China): miR-590-3p: forward 5′-CGGGGGTAATTTTATGTATAAGCTAGT-3′ and reverse 5′-CTCAACTGGTGTCGTGGA-3′; U6: forward 5′-CTCGCTTCGGCAGCACA-3′ and reverse 5′-AACG CTTCACGAATTTGCGT-3′; TRAF6: forward 5′-GCCG AAATGGAAGCACAG-3′ and reverse 5′-CAGG GCTATGGATGACAACA-3′; GAPDH: forward 5′-GCACCGTCAAGCTGAGAAC-3′ and reverse 5′-TGGT GAAGACGCCAGTGGA-3′.

WESTERN BLOTTING

Proteins were extracted with radio immunoprecipitation assay (RIPA) buffer (cat. No: P0013B; Beyotime Institute of Biotechnology) with protease inhibitors, and the concentrations were determined using the Bicinchoninic Acid Kit for Protein Determination (cat. no: BCA1-1KT; Sigma-Aldrich; Merck KGaA). Thirty micrograms of protein for each sample was separated on a 10% SDS-PAGE gel and transferred to nitrocellulose membranes (Bio-Rad Laboratories, Inc., Hercules, CA, USA). The membranes were incubated with the primary antibodies TRAF6 (cat. no: sc-8409; dilution: 1:1000; Santa Cruz Biotechnology, Santa Cruz, CA, USA), TNF-α (cat. no: sc-52746; dilution: 1:1000; Santa Cruz Biotechnology), IL-1β (cat. no: ab150777; dilution: 1:1000; Abcam), IL-6 (cat. no: sc-32296; dilution: 1:1000; Santa Cruz Biotechnology), TLR4 (cat. no: sc-293072; dilution: 1:500; Santa Cruz Biotechnology, Santa Cruz, CA, USA), NF-κB/p65 (cat. no: 3034; dilution: 1:500; Cell Signaling Technology, Inc., USA), or cleaved-caspase3 (cat. no: 9661; dilution: 1:2000; Cell Signaling Technology, USA) at room temperature for 2 h. β-actin (cat. no: sc-130301; dilution: 1:2000; Santa Cruz Biotechnology) signals were used to correct for unequal loading. Following three washes with TBST, the membranes were incubated with the appropriate horseradish peroxidase-conjugated secondary antibody (cat. no: sc-516102; dilution: 1:10,000; Santa Cruz Biotechnology) at room temperature for 2 h and visualized by chemiluminescence (Thermo Fisher Scientific, Inc.). Signals were analyzed with Quantity One® software version 4.5 (Bio-Rad Laboratories, Inc., Hercules, CA, USA).

Immunohistochemical Staining

Renal tissues were embedded with paraffin and were cut into 3-μm sections. Immunohistochemical staining was performed as described previously [45]. Briefly, the section was incubated with the TRAF6 primary antibody (cat. no: sc-8409; dilution: 1:50; Santa Cruz Biotechnology) and treated with the ABC staining system (Santa Cruz Biotechnology). A microscope (Leica DM 2500; Leica Microsystems GmbH, Wetzlar, Germany) and image Pro-Plus 6 software (Media Cybernetics, Inc., Rockville, MD, USA) was used for the integrated optical density analysis.

Statistical Analysis

Data were presented as the mean ± standard deviation for each group. All statistical analyses were performed using PRISM version 7.0 (GraphPad Software, Inc., La Jolla, CA, USA). Intergroup differences were analyzed by one-way analysis of variance, followed by a *post hoc* Tukey test for multiple comparisons. A P value < 0.05 was considered to indicate a statistically significant difference.

RESULTS

Ad-miR-590-3p Improves Survival Outcome in LPS-Treated Mice

We observed the 96-h survival of control, LPS, LPS with ad-miR-con, or LPS with ad-miR-590-3p-treated mice. The results showed that LPS induced a poor survival outcome and a 100% mortality occurred within 70 h after LPS treatment, while LPS-treated mice with ad-miR-590-3p *via* tail-vein injection significantly improved survival outcomes with a 40% survival rate (Fig. 1).

Ad-miR-590-3p Alleviates AKI and Inflammatory Response in LPS-Administered Mice

To investigate the effects of miR-590-3p on LPS-induced AKI and the inflammatory response *in vivo*, we administered ad-miR-590-3p and ad-miR-Con *via* tail-vein injection to male C57BL/6J mice and found that miR-590-3p levels were significantly increased in the kidneys of those septic mice injected with ad-miR-590-

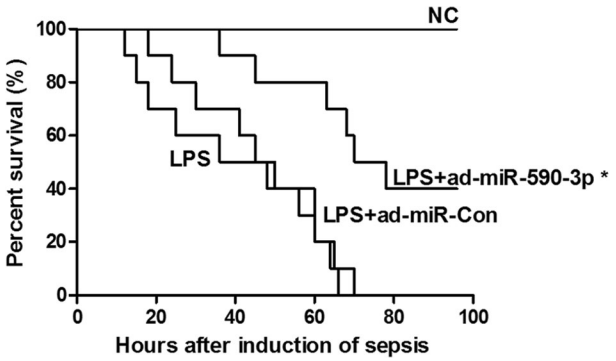

Fig. 1. Ad-miR-590-3p improves survival outcome in LPS-treated mice. Ad-miR-590-3p or ad-miR-Con was transfected into LPS-induced mice, ad-miR-590-3p significantly improved survival outcome in septic mice. $^{*}P < 0.05$, compared with LPS + ad-miR-Con group. $n = 10$ in each group.

3p when compared with the ad-miR-Con group (Fig. 2a). To investigate the effects of miR-590-3p on AKI, we analyzed the renal GFR by measuring serum CysC, serum β2-MG, and BUN under different treatment conditions. As shown in Fig. 2b–d, all these measurements were significantly higher in LPS-treated mice than in healthy control mice, while injecting ad-miR-590-3p significantly reduced the increase of CysC, β2-MG and BUN in septic mice. We further investigated whether injection of ad-miR-590-3p was correlated with decreased proinflammatory mediators. Proinflammatory mediators TNF-α, IL-1β, and IL-6 contribute to sepsis-induced renal injury [2]. We determined that LPS resulted in a significant increase in TNF-α, IL-1β, and IL-6 in the serum of septic mice, which could be markedly attenuat-

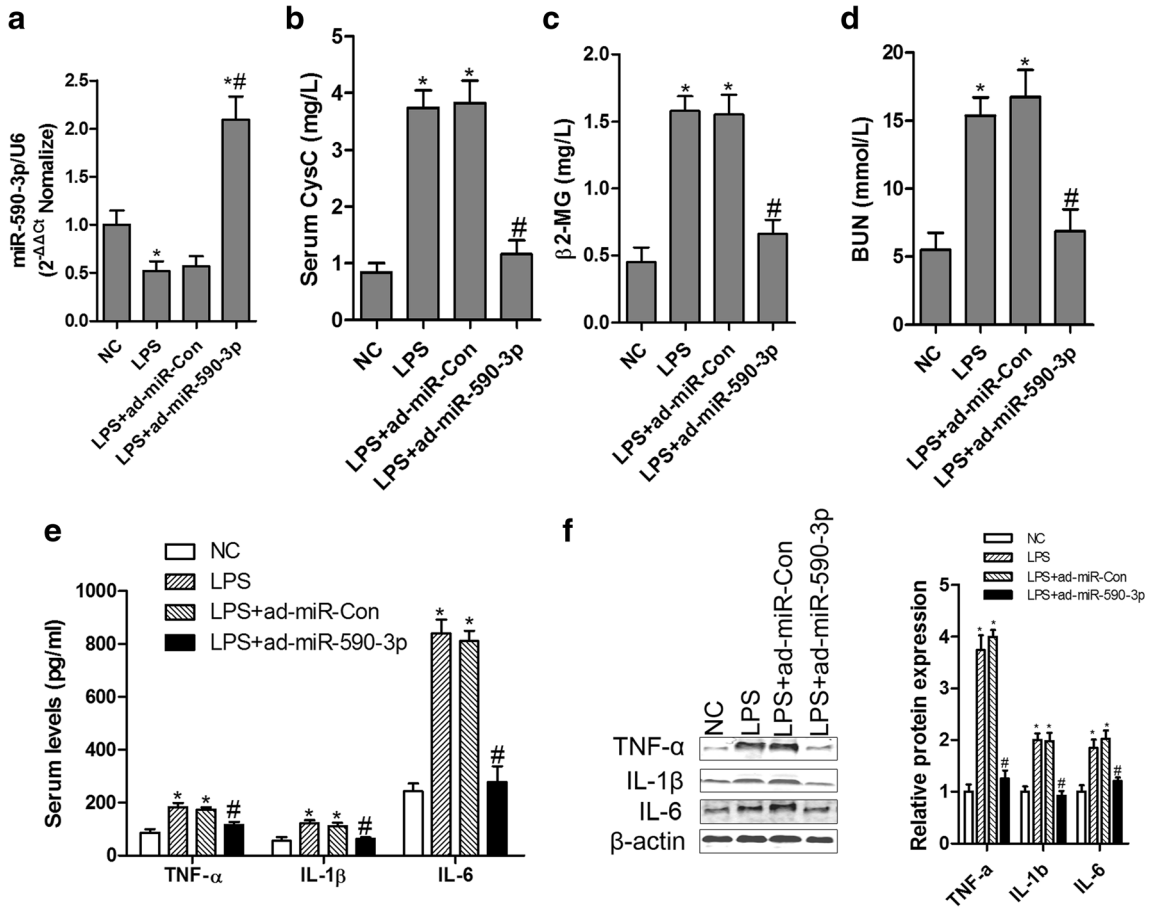

Fig. 2. Ad-miR-590-3p alleviates AKI and inflammatory response in LPS-administrated mice. After transfected with ad-miR-590-3p or ad-miR-Con into LPS-treated mice, the levels of miR-590-3p were performed by RT-qPCR (**a**); serum cystatin C (CysC, **b**), β2-microglobulin (β2-MG, **c**) and blood urea nitrogen (BUN, **d**) were measured by ELISA assay. The serum levels of inflammatory cytokines, tumor necrosis factor α (TNF-α), interleukin-1β (IL-1β), and interleukin 6 (IL-6) were measured by mouse ELISA kit (**e**). The protein expression of TNF-α, IL-1β, and IL-6 in the kidney was detected by western blotting (**f**). $^{*}P < 0.05$, compared with NC group; $^{\#}P < 0.05$, compared with LPS + ad-miR-Con group. $n = 10$ in each group.

ed by the ad-miR-590-3p treatment (Fig. 2e). Moreover, our *in vivo* data demonstrated that injection of ad-miR-590-3p significantly attenuated LPS-induced TNF-α, IL-1β, and IL-6 protein expression in the kidneys when compared to the expression in the ad-miR-Con group (Fig. 2f). We have shown above that the decrease in the proinflammatory mediators, TNF-α, IL-1β, and IL-6, and the improvement of AKI might contribute to the elevated survival rate after ad-miR-590-3p injection.

Ad-miR-590-3p Suppresses TRAF6 Expression in the Kidney

TRAF6 is an important component in TLR/IL-1 receptor-mediated NF-κB activation, which regulates the expression of inflammatory cytokines and adhesion molecules [27]. To explain the correlation between miR-590-3p and TRAF6-related inflammatory cytokines, we further verified the presence of TRAF6 and the changes of its expression in the kidneys from septic mice by RT-qPCR (Fig. 3a), western blotting (Fig. 3b), and immunohistochemical staining (Fig. 3c). As shown in Fig. 3a–c, TRAF6 was substantially expressed in the kidneys of septic mice; however, injection of ad-miR-590-3p weakened the TRAF6 signaling in the kidney compared with that of the ad-miR-Con group. In addition, western blotting assay indicated that the LPS-amplified protein expression of TLR4 and nucleic NF-κB/p65 was markedly attenuated by the injection of ad-miR-590-3p (Fig. 3d). Therefore, it is possible that miR-590-3p improved LPS-induced AKI and inflammatory responses, at least partially, through the suppression of the TLR4/TRAF6/NF-κB signaling pathway.

TRAF6 Is a Direct Target of miR-590-3p

To investigate whether TRAF6 was a direct target of miR-590-3p, the online prediction software miRanda was used. The results demonstrated that the 3′-UTR of TRAF6 contained one conserved miR-590-3p binding site (Fig. 4a). To confirm this, a pGL3-promoter-based TRAF6 3′-UTR was cotransfected with mimics or control sequences of miR-590-3p into podocytes. When compared to the NC group, the luciferase activity with the TRAF6 3′-UTR was significantly inhibited by miR-590-3p mimics, but the luciferase activity had no change with the mutated TRAF6 3′-UTR reporter by mimics or control sequences of miR-590-3p transfection (Fig. 4b). We also found that overexpression of miR-590-3p significantly inhibited both the mRNA and protein expression of TRAF6 compared to the control group (Fig. 4c, d).

Overexpression of miR-590-3p Inhibits LPS-Induced Cell Growth Inhibition and Apoptosis

Previous studies have shown that LPS is a potent stimulus for apoptosis of podocytes [42]. Consistent with previous result, our study demonstrated that podocyte viability was inhibited by LPS in a time- and concentration-dependent manner (Fig. 5a), which might be associated with LPS-induced cell apoptosis in podocytes. Next, the apoptosis was analyzed in LPS-treated podocytes; the results suggested that LPS induced podocyte apoptosis in a concentration-dependent manner (Fig. 5b, c). Furthermore, LPS administration resulted in a significant increase in cleaved-caspase3 protein expression (Fig. 5d). Intriguingly, LPS-induced cell growth inhibition (Fig. 6a), apoptosis (Fig. 6b, c), and upregulation of cleaved-caspase3 protein expression (Fig. 6d) in podocytes were reversed by transfection with miR-590-3p mimics.

Overexpression of miR-590-3p Inhibits TLR4/TRAF6/NF-κB Inflammatory Signaling

To further investigate the underlying molecular mechanisms of LPS-induced apoptosis in podocytes, the expression of TLR4, TRAF6, and NF-κB/p65 in the nucleus was detected in LPS-stimulated podocytes. Western blotting confirmed that TLR4, TRAF6, and nucleic NF-κB-p65 were markedly increased in LPS-stimulated podocytes; however, overexpression of miR-590-3p blocked the LPS-induced activation of the TLR4/TRAF6/NF-κB inflammatory signaling pathway (Fig. 7a, b). In addition, we detected that the levels of the proinflammatory mediators, TNF-α, IL-1β, and IL-6, in the culture supernatant after treatment with LPS or miR-590-3p mimicked transfection. The increase in proinflammatory cytokines, TNF-α, IL-1β, and IL-6, in LPS-treated podocytes, was alleviated by the overexpression of miR-590-3p (Fig. 7c).

DISCUSSION

Previous studies indicated that miR-590 family members have been implicated in oxidized low-density lipoprotein- and chitinase-3-like-1-induced aseptic inflammatory responses [6, 11, 12, 16]. In addition, the suppression of miR-590-3p is accompanied with the promotion of interleukin-18 expression [16]. In our study, we concentrated on investigating the role of miR-590-3p in LPS-induced AKI and inflammation. A direct effect of miR-590-3p on sepsis-induced inflammatory response has not been described previously. We observed that the levels of miR-

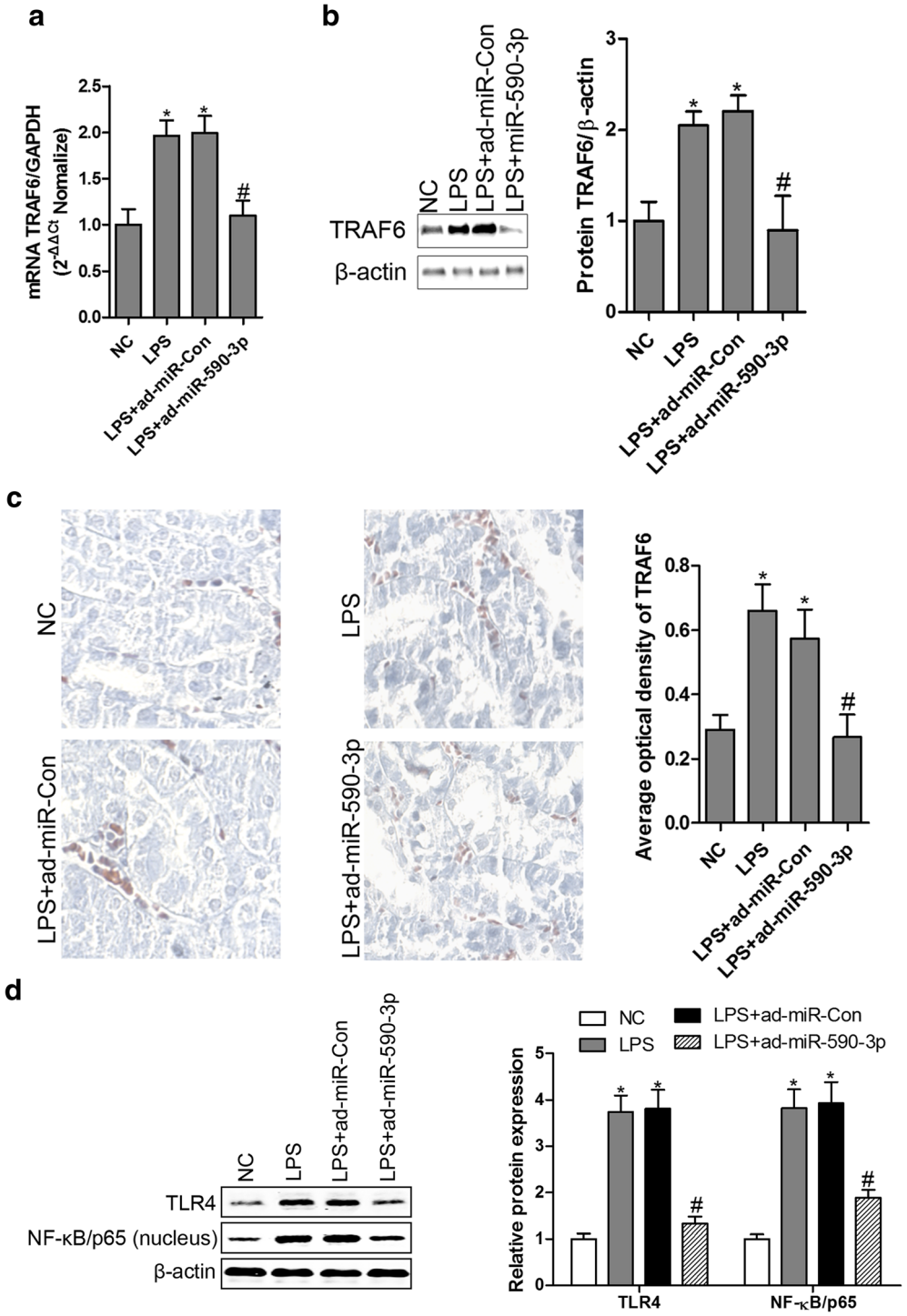

Fig. 3. Ad-miR-590-3p suppresses TRAF6 expression in the kidney. After transfected with ad-miR-590-3p or ad-miR-Con into LPS-treated mice, the mRNA (**a**) and protein (**b**) expression of TRAF6 were performed by RT-qPCR and western blotting, respectively. TRAF6 expression in the kidneys was performed by immunohistochemical staining (**c**). The protein expression of TLR4 and NF-κB/p65 was measured by western blotting (**d**). $^{*}P < 0.05$, compared with NC group; $^{\#}P < 0.05$, compared with LPS + ad-miR-Con group. $n = 10$ in each group.

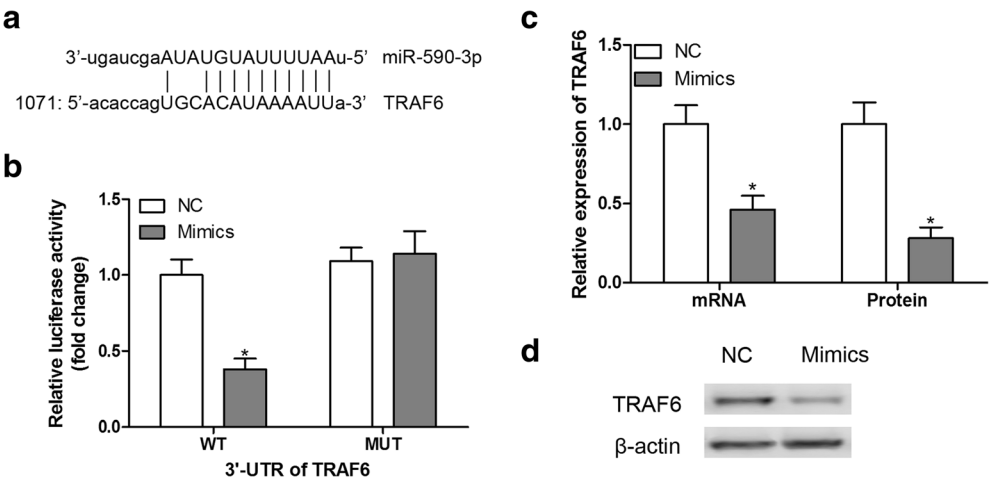

Fig. 4. TRAF6 is a direct target of miR-590-3p. Schematic representation of the putative miR-590-3p binding site in the 3′UTR of TRAF6 was predicted by the online database (**a**). The podocytes were cotransfected with the WT and MUT of TRAF6-3′-UTR and miR-590-3p mimics or miR-Con, and the luciferase activity assay was performed (**b**). After transfected with miR-590-3p mimics, the mRNA and protein expression of TRAF6 were performed by RT-qPCR and western blotting, respectively (**c**, **d**). $^{*}P < 0.05$, compared with NC group. $n = 3$ in each group.

590-3p were markedly decreased in the kidneys from LPS-treated mice. However, ad-miR-590-3p-injected mice exhibited inhibitions of systematic and local inflammatory responses, indicating that miR-590-3p might play an important role in the negative regulation of the inflammatory response to septic challenge. A posttranscriptional

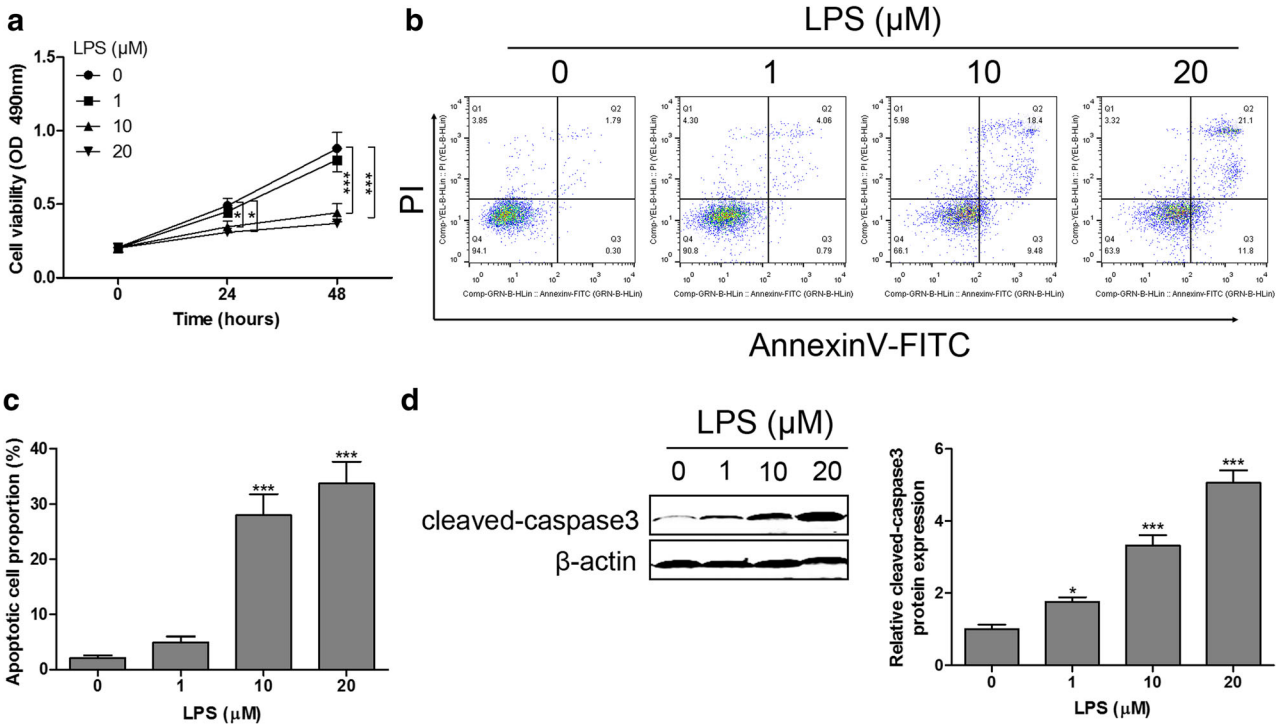

Fig. 5. LPS induces apoptosis and inhibits growth in podocyte. Podocytes were exposed to LPS (0, 1, 10, and 20 μM) for 0–48 h, cell viability was measured by MTT assay (**a**). Podocytes exposed to LPS (0, 1, 10, and 20 μM) for 48 h, podocyte apoptosis was measured by flow cytometry (**b**, **c**); the protein expression of cleaved-caspase3 was measured by western blotting (**d**). $^{*}P < 0.05$; $^{***}P < 0.001$ compared with control group. $n = 3$ in each group.

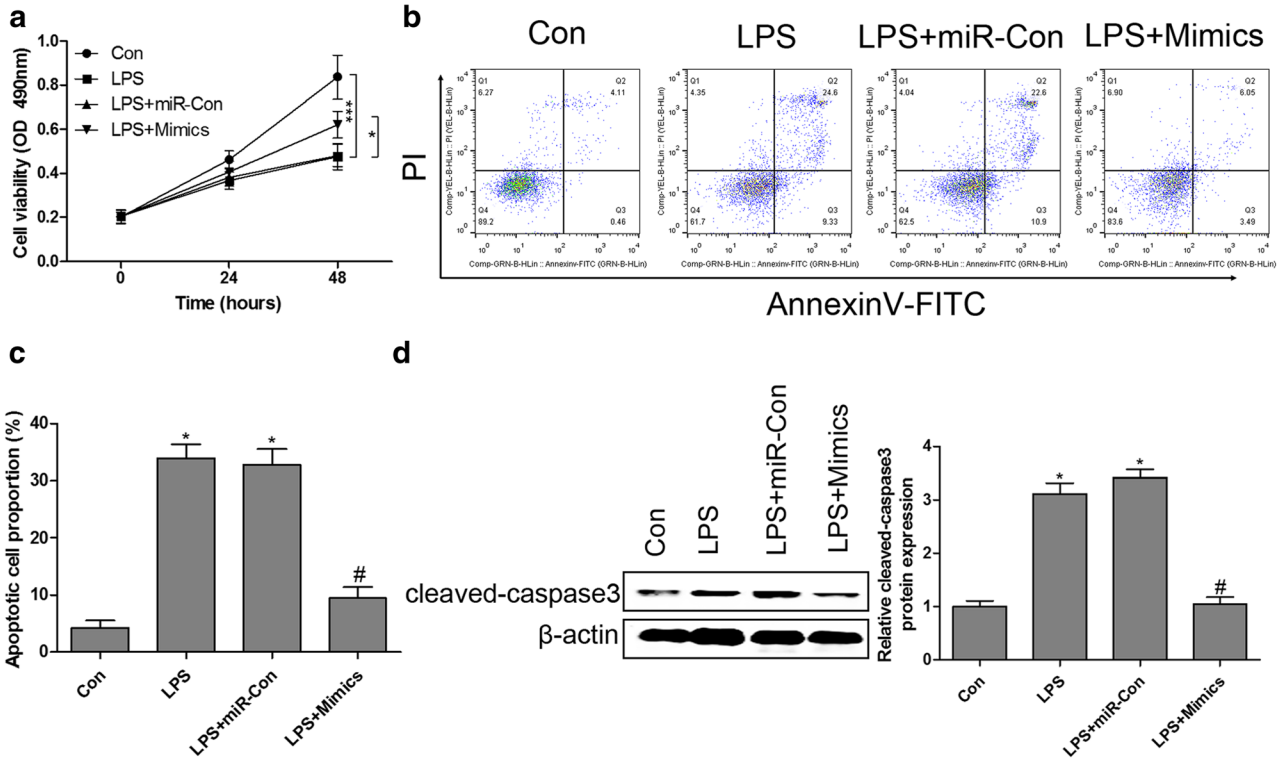

Fig. 6. Overexpression of miR-590-3p inhibits LPS-induced cell growth inhibition and apoptosis. After transfected with miR-Con and miR-590-3p mimics for 48 h, cell viability was measured by MTT assay (**a**); podocyte apoptosis was measured by flow cytometry (**b**, **c**); the protein expression of cleaved-caspase3 was measured by western blotting (**d**). $^{*}P < 0.05$; $^{***}P < 0.001$ compared with control group; $^{\#}P < 0.05$ compared with LPS + miR-Con group. $n = 3$ in each group.

regulatory mechanism suggested that miR-590-3p inhibition could target the expression of TRAF6 and TLR4/TRAF6/NF-κB inflammatory signaling-mediated apoptosis and the upregulation of proinflammatory cytokines levels in LPS-treated podocytes or mice. These findings uncovered that LPS-induced podocyte apoptosis *in vitro* and AKI *in vivo* could be attenuated by overexpressed miR-590-3p, and the underlying mechanism was mediated, at least partially, through the inactivation of TLR4/TRAF6/NF-κB inflammatory signaling (Fig. 8).

To investigate whether the upregulation of miR-590-3p could improve survival outcomes of LPS-induced sepsis, we infected mice with ad-miR-590-3p *via* tail-vein injection. We found that in LPS-treated mice miR-590-3p injection significantly attenuated AKI and improved survival outcomes following LPS-induced sepsis. Previous studies have reported that the TRAF6-involved inflammatory response contributes to the pathophysiology of LPS-induced sepsis [17, 46]. Therefore, the activation of the TRAF6 pathway could be a potential therapeutic target for sepsis-related organ injury.

Our data confirmed that TRAF6 was a target gene of miR-590-3p. Indeed, published *in vitro* and *in vivo* data by others have shown that several miRs, including miR-124, miR-126, miR-144, miR-146a, and miR-146b-5p, can target to the TRAF6 pathway [19, 28, 31, 39, 44]. Previous studies indicated that inhibition of TRAF6 by miR-125b mimics markedly suppress inflammatory responses mediated by NF-κB and MAPK signaling [27]. In addition, miR-146a regulates inflammatory macrophage infiltration *via* the targeting of TRAF6 and affecting the IL-17/intercellular adhesion molecule 1 pathway [44]. Consistent with these findings, the present study showed that *in vivo* ad-miR-590-3p transfection reduced renal TRAF6 expression as well as nucleic NF-κB-p65. Collectively, previous data [27, 44] and the current study suggest that inhibition of TRAF6 by miRs may be an important approach for the attenuation of LPS-induced pathological changes of tissues.

A recent study showed that miR-590-3p is aberrantly expressed in experimental autoimmune myocarditis and that miR-590-3p transfection through adeno-associated virus significantly inhibits NF-κB activity, blocks IL-6/TNF-α

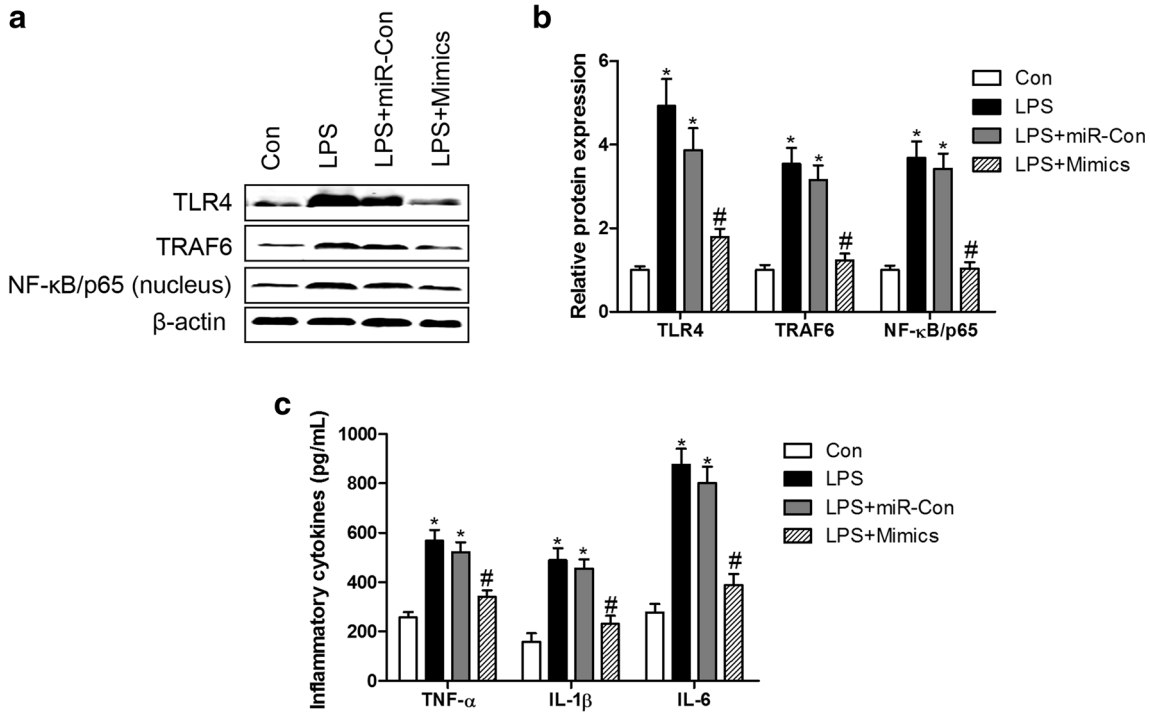

Fig. 7. Overexpression of miR-590-3p inhibits TLR4/TRAF6/NF-κB inflammatory signaling. After transfected with miR-Con and miR-590-3p mimics for 48 h, the protein expression of TLR4, TRAF6, and NF-κB/p65 in the nucleus was detected by western blotting (**a**, **b**); proinflammatory mediators, TNF-α, IL-1β, and IL-6, in the culture supernatant were measured by ELISA assay (**c**). $^{*}P < 0.05$ compared with control group; $^{\#}P < 0.05$ compared with LPS + miR-Con group. $n = 3$ in each group.

expression, and improves cardiac function *in vivo* [49], suggesting that miR-590-3p may be involved in the regulation of the inflammatory response. Consistent with the role of miR-590-3p, other studies have shown that miR-590-3p exerts opposite influences on IL-18 in endothelial progenitor cells [16]. Our findings also showed a significant downregulation of the local kidney and circulation TNF-α, IL-1β, and IL-6 levels, suggesting that the importance of miR-590-3p in LPS-induced AKI should not be ignored.

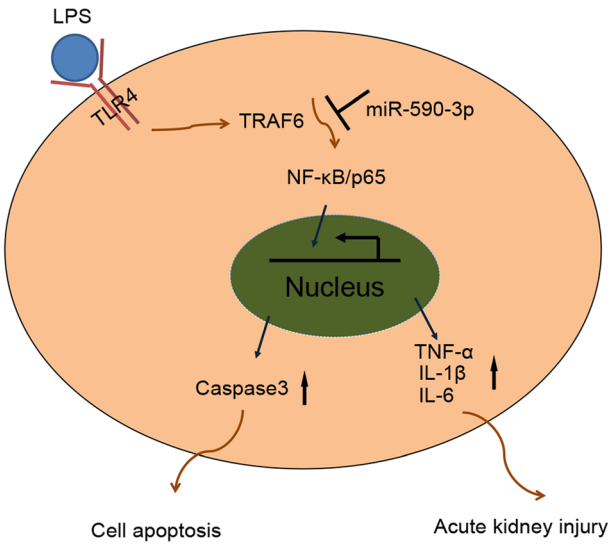

Fig. 8. A simplified model for how the miR-590-3p mediated the suppression of LPS-induced AKI and podocyte apoptosis by targeting TLR4/TRAF6/NF-κB cascade signaling.

Our results also found that overexpressed miR-590-3p inhibited LPS-evoked podocyte apoptosis and TLR4/TRAF6/NF-κB inflammatory signaling *in vitro*. Podocytes are a kind of glomerular epithelial cell with high specialization and terminal differentiation and attach to the outside of the glomerular basement membrane, which plays a crucial role in maintaining the integrity of the glomerular filtration barrier [26, 50]. A previous study showed that podocyte apoptosis is closely related with AKI in a mouse sepsis model [30]. TLR4/NF-κB signaling may be a potential molecular target for attenuating high glucose or endotoxemia-induced podocyte dysfunction and apoptosis [20, 36, 43]. The present study revealed that miR-590-3p as a posttranscriptional regulator blocked LPS-induced podocyte apoptosis by inhibiting

TLR4/TRAF6/NF-κB inflammatory pathway, which might provide an alternative mechanism to improve AKI development in septic mice.

Gene therapy has become well accepted in clinical practice [8]. The delivery strategies of gene therapy include adenovirus, lentivirus, lipid nanoparticles, polymeric nanoparticles, and microvesicles [29]. For example, Xiao et al. recently reported that adenovirus-mediated overexpression of miR-130a-3p reverses insulin resistance and liver steatosis [41]. Liu et al. described a microvesicle-based method that neutralizes miR-150 and attenuates tumor development [21]. In the present study, adenovirus-delivered miR-590-3p into the renal tissues efficiently repressed LPS-induced AKI, further suggesting that adenovirus-delivered small RNAs are advantageous carriers for gene therapy.

In summary, this is the first *in vivo* study indicating that adenovirus-delivered miR-590-3p can be shuttled into the kidneys to downregulate TRAF6 expression and inhibit inflammatory cytokine expression. Our results are also important in providing a new perspective for the understanding of the underlying molecular mechanisms and potential therapeutic target for LPS-induced AKI.

ACKNOWLEDGMENTS

We give thanks to the Department of Pathology, Wuhan Third Hospital of Wuhan University to provide technical support.

COMPLIANCE WITH ETHICAL STANDARDS

The experiment was approved by the Ethics Committee of the Wuhan three hospital of Wuhan University (Wuhan, China) and performed in accordance with its guidelines.

Conflict of Interest. The authors declare that they have no competing interests.

REFERENCES

1. An, R., J. Feng, C. Xi, and J. Xu. 2018. miR-146a attenuates sepsis-induced myocardial dysfunction by suppressing IRAK1 and TRAF6 via targeting ErbB4 expression. *Oxidative Medicine and Cellular Longevity* 2018: 7163057: 1–9.
2. Bhargava, R., C.J. Altmann, A. Andres-Hernando, R.G. Webb, K. Okamura, Y. Yang, S. Falk, E.P. Schmidt, and S. Faubel. 2013. Acute lung injury and acute kidney injury are established by four hours in experimental sepsis and are improved with pre, but not post, sepsis administration of TNF-alpha antibodies. *PLoS One* 8: e79037.
3. Chen, C., Z. Liang, W. Huang, X. Li, F. Zhou, X. Hu, M. Han, X. Ding, and S. Xiang. 2015. Eps8 regulates cellular proliferation and migration of breast cancer. *International Journal of Oncology* 46: 205–214.
4. Chen, F., S. He, R. Qiu, R. Pang, J. Xu, and J. Dong. 2010. Influence of silencing TRAF6 with shRNA on LPS/TLR4 signaling in vitro. *Journal of Huazhong University of Science and Technology. Medical Sciences* 30: 278–284.
5. Dai, Y., P. Jia, Y. Fang, H. Liu, X. Jiao, J.C. He, and X. Ding. 2016. miR-146a is essential for lipopolysaccharide (LPS)-induced cross-tolerance against kidney ischemia/reperfusion injury in mice. *Scientific Reports* 6: 27091.
6. Dai, Y., Z. Zhang, Y. Cao, J.L. Mehta, and J. Li. 2016. MiR-590-5p inhibits oxidized- LDL induced angiogenesis by targeting LOX-1. *Scientific Reports* 6: 22607.
7. Emmerich, C.H., A. Ordureau, S. Strickson, J.S. Arthur, P.G. Pedrioli, D. Komander, and P. Cohen. 2013. Activation of the canonical IKK complex by K63/M1-linked hybrid ubiquitin chains. *Proceedings of the National Academy of Sciences of the United States of America* 110: 15247–15252.
8. Fischer, A. 2014. Gene therapy: Repair and replace. *Nature* 510: 226–227.
9. Gao, M., X. Wang, X. Zhang, T. Ha, H. Ma, L. Liu, J.H. Kalbfleisch, X. Gao, R.L. Kao, D.L. Williams, and C. Li. 2015. Attenuation of cardiac dysfunction in polymicrobial sepsis by microRNA-146a is mediated via targeting of IRAK1 and TRAF6 expression. *Journal of Immunology* 195: 672–682.
10. He, A., R. Ji, J. Shao, C. He, M. Jin, and Y. Xu. 2016. TLR4-MyD88-TRAF6-TAK1 complex-mediated NF-kappaB activation contribute to the anti-inflammatory effect of V8 in LPS-induced human cervical cancer SiHa cells. *Inflammation* 39: 172–181.
11. He, P.P., X.P. Ouyang, Y.Y. Tang, L. Liao, Z.B. Wang, Y.C. Lv, G.P. Tian, G.J. Zhao, L. Huang, F. Yao, W. Xie, Y.L. Tang, W.J. Chen, M. Zhang, Y. Li, J.F. Wu, J. Peng, X.Y. Liu, X.L. Zheng, W.D. Yin, and C.K. Tang. 2014. MicroRNA-590 attenuates lipid accumulation and pro-inflammatory cytokine secretion by targeting lipoprotein lipase gene in human THP-1 macrophages. *Biochimie* 106: 81–90.
12. Karagiannis, G.S., J. Weile, G.D. Bader, and J. Minta. 2013. Integrative pathway dissection of molecular mechanisms of moxLDL-induced vascular smooth muscle phenotype transformation. *BMC Cardiovascular Disorders* 13: 4.
13. Lee, Y., I.Y. Lee, H.J. Yun, W.S. Lee, S. Kang, S.G. Cho, J.E. Lee, and E.J. Choi. 2016. BAT3 negatively regulates lipopolysaccharide-induced NF-kappaB signaling through TRAF6. *Biochemical and Biophysical Research Communications* 478: 784–790.
14. Li, H.R., J. Liu, S.L. Zhang, T. Luo, F. Wu, J.H. Dong, Y.J. Guo, and L. Zhao. 2017. Corilagin ameliorates the extreme inflammatory status in sepsis through TLR4 signaling pathways. *BMC Complementary and Alternative Medicine* 17: 18.
15. Li, N., H. Xie, L. Li, J. Wang, M. Fang, N. Yang, and H. Lin. 2014. Effects of honokiol on sepsis-induced acute kidney injury in an experimental model of sepsis in rats. *Inflammation* 37: 1191–1199.
16. Li, T.M., S.C. Liu, Y.H. Huang, C.C. Huang, C.J. Hsu, C.H. Tsai, S.W. Wang, and C.H. Tang. 2017. YKL-40-induced inhibition of miR-590-3p promotes interleukin-18 expression and angiogenesis of endothelial progenitor cells. *International Journal of Molecular Sciences* 18.

17. Li, X.M., S. Zhang, X.S. He, P.D. Guo, X.X. Lu, J.R. Wang, J.M. Li, and H. Wu. 2016. Nur77-mediated TRAF6 signalling protects against LPS-induced sepsis in mice. *J Inflamm (Lond)* 13: 4.
18. Lin, X., S. Steinberg, S.K. Kandasamy, J. Afzal, B. Mbiyangandu, S.E. Liao, Y. Guan, et al. 2016. Common miR-590 variant rs6971711 present Only in African Americans reduces miR-590 biogenesis. *PLoS One* 11: e0156065.
19. Liu, J., J. Xu, H. Li, C. Sun, L. Yu, Y. Li, C. Shi, et al. 2015. miR-146b-5p functions as a tumor suppressor by targeting TRAF6 and predicts the prognosis of human gliomas. *Oncotarget* 6: 29129–29142.
20. Liu, Y., Z. Xu, F. Ma, Y. Jia, and G. Wang. 2018. Knockdown of TLR4 attenuates high glucose-induced podocyte injury via the NALP3/ASC/Caspase-1 signaling pathway. *Biomedicine & Pharmacotherapy* 107: 1393–1401.
21. Liu, Y., L. Zhao, D. Li, Y. Yin, C.Y. Zhang, J. Li, and Y. Zhang. 2013. Microvesicle-delivery miR-150 promotes tumorigenesis by up-regulating VEGF, and the neutralization of miR-150 attenuate tumor development. *Protein & Cell* 4: 932–941.
22. Livak, K.J., and T.D. Schmittgen. 2001. Analysis of relative gene expression data using real-time quantitative PCR and the 2(-Delta Delta C(T)) Method. *Methods* 25: 402–408.
23. Lopes, J.A., P. Fernandes, S. Jorge, C. Resina, C. Santos, A. Pereira, J. Neves, F. Antunes, and A. Gomes da Costa. 2010. Long-term risk of mortality after acute kidney injury in patients with sepsis: A contemporary analysis. *BMC Nephrology* 11: 9.
24. Loubaki, L., D. Chabot, I. Pare, M. Drouin, and R. Bazin. 2017. MiR-146a potentially promotes IVIg-mediated inhibition of TLR4 signaling in LPS-activated human monocytes. *Immunology Letters* 185: 64–73.
25. Lv, F., Y. Huang, W. Lv, L. Yang, F. Li, J. Fan, and J. Sun. 2017. MicroRNA-146a ameliorates inflammation via TRAF6/NF-kappaB pathway in intervertebral disc cells. *Medical Science Monitor* 23: 659–664.
26. Lv, Z., M. Hu, M. Fan, X. Li, J. Lin, J. Zhen, Z. Wang, H. Jin, and R. Wang. 2018. Podocyte-specific Rac1 deficiency ameliorates podocyte damage and proteinuria in STZ-induced diabetic nephropathy in mice. *Cell Death & Disease* 9: 342.
27. Ma, H., X. Wang, T. Ha, M. Gao, L. Liu, R. Wang, K. Yu, J.H. Kalbfleisch, R.L. Kao, D.L. Williams, and C. Li. 2016. MicroRNA-125b prevents cardiac dysfunction in polymicrobial sepsis by targeting TRAF6-mediated nuclear factor kappaB activation and p53-mediated apoptotic signaling. *The Journal of Infectious Diseases* 214: 1773–1783.
28. Meng, Q., W. Zhang, X. Xu, J. Li, H. Mu, X. Liu, L. Qin, X. Zhu, and M. Zheng. 2018. The effects of TRAF6 on proliferation, apoptosis and invasion in osteosarcoma are regulated by miR-124. *International Journal of Molecular Medicine* 41: 2968–2976.
29. Pan, S., X. Yang, Y. Jia, Y. Li, R. Chen, M. Wang, D. Cai, and R. Zhao. 2015. Intravenous injection of microvesicle-delivery miR-130b alleviates high-fat diet-induced obesity in C57BL/6 mice through translational repression of PPAR-gamma. *Journal of Biomedical Science* 22: 86.
30. Peng, Y., X. Zhang, Y. Wang, S. Li, J. Wang, and L. Liu. 2015. Overexpression of toll-like receptor 2 in glomerular endothelial cells and podocytes in septic acute kidney injury mouse model. *Renal Failure* 37: 694–698.
31. Rosenberger, C.M., R.L. Podyminogin, A.H. Diercks, P.M. Treuting, J.J. Peschon, D. Rodriguez, M. Gundapuneni, M.J. Weiss, and A. Aderem. 2017. miR-144 attenuates the host response to influenza virus by targeting the TRAF6-IRF7 signaling axis. *PLoS Pathogens* 13: e1006305.
32. Souza, A.C., P.S. Yuen, and R.A. Star. 2015. Microparticles: markers and mediators of sepsis-induced microvascular dysfunction, immunosuppression, and AKI. *Kidney International* 87: 1100–1108.
33. Stickel, N., G. Prinz, D. Pfeifer, P. Hasselblatt, A. Schmitt-Graeff, M. Follo, R. Thimme, J. Finke, J. Duyster, U. Salzer, and R. Zeiser. 2014. MiR-146a regulates the TRAF6/TNF-axis in donor T cells during GVHD. *Blood* 124: 2586–2595.
34. Sun, G., W. Yang, Y. Zhang, and M. Zhao. 2017. Esculentoside A ameliorates cecal ligation and puncture-induced acute kidney injury in rats. *Experimental Animals* 66: 303–312.
35. Walsh, M.C., J. Lee, and Y. Choi. 2015. Tumor necrosis factor receptor- associated factor 6 (TRAF6) regulation of development, function, and homeostasis of the immune system. *Immunological Reviews* 266: 72–92.
36. Wei, M., Z. Li, L. Xiao, and Z. Yang. 2015. Effects of ROS-relative NF-kappaB signaling on high glucose-induced TLR4 and MCP-1 expression in podocyte injury. *Molecular Immunology* 68: 261–271.
37. Wu, S., W. Liu, and L. Zhou. 2016. MiR-590-3p regulates osteogenic differentiation of human mesenchymal stem cells by regulating APC gene. *Biochemical and Biophysical Research Communications* 478: 1582–1587.
38. Wu, T., Y. Xiang, Y. Lv, D. Li, L. Yu, and R. Guo. 2017. miR-590-3p mediates the protective effect of curcumin on injured endothelial cells induced by angiotensin II. *American Journal of Translational Research* 9: 289–300.
39. Wu, Y., L.T. Song, J.S. Li, D.W. Zhu, S.Y. Jiang, and J.Y. Deng. 2017. MicroRNA-126 regulates inflammatory cytokine secretion in human gingival fibroblasts under high glucose via targeting tumor necrosis factor receptor associated factor 6. *Journal of Periodontology* 88: e179–e187.
40. Xiao, F., Z. Huang, H. Li, J. Yu, C. Wang, S. Chen, Q. Meng, Y. Cheng, X. Gao, J. Li, Y. Liu, and F. Guo. 2011. Leucine deprivation increases hepatic insulin sensitivity via GCN2/mTOR/S6K1 and AMPK pathways. *Diabetes* 60: 746–756.
41. Xiao, F., J. Yu, B. Liu, Y. Guo, K. Li, J. Deng, J. Zhang, C. Wang, S. Chen, Y. du, Y. Lu, Y. Xiao, Z. Zhang, and F. Guo. 2014. A novel function of microRNA 130a-3p in hepatic insulin sensitivity and liver steatosis. *Diabetes* 63: 2631–2642.
42. Xu, L., P. Zhang, H. Guan, Z. Huang, X. He, X. Wan, H. Xiao, and Y. Li. 2016. Vitamin D and its receptor regulate lipopolysaccharide-induced transforming growth factor-beta, angiotensinogen expression and podocytes apoptosis through the nuclear factor-kappaB pathway. *Journal of Diabetes Investigation* 7: 680–688.
43. Xu, M.X., M. Wang, and W.W. Yang. 2017. Gold-quercetin nanoparticles prevent metabolic endotoxemia-induced kidney injury by regulating TLR4/NF-kappaB signaling and Nrf2 pathway in high fat diet fed mice. *International Journal of Nanomedicine* 12: 327–345.
44. Yin, Y., F. Li, J. Shi, S. Li, J. Cai, and Y. Jiang. 2016. MiR-146a regulates inflammatory infiltration by macrophages in polymyositis/dermatomyositis by targeting TRAF6 and affecting IL-17/ICAM-1 pathway. *Cellular Physiology and Biochemistry* 40: 486–498.
45. Zapata, J.M., M. Krajewska, S. Krajewski, S. Kitada, K. Welsh, A. Monks, N. McCloskey, J. Gordon, T.J. Kipps, R.D. Gascoyne, A. Shabaik, and J.C. Reed. 2000. TNFR-associated factor family protein expression in normal tissues and lymphoid malignancies. *Journal of Immunology* 165: 5084–5096.
46. Zeng, K.W., L.X. Liao, H.N. Lv, F.J. Song, Q. Yu, X. Dong, J. Li, Y. Jiang, and P.F. Tu. 2015. Natural small molecule FMHM inhibits lipopolysaccharide-induced inflammatory response by promoting TRAF6 degradation via K48-linked polyubiquitination. *Scientific Reports* 5: 14715.

47. Zhang, J., G. Ankawi, J. Sun, K. Digvijay, Y. Yin, M.H. Rosner, and C. Ronco. 2018. Gut-kidney crosstalk in septic acute kidney injury. *Critical Care* 22: 117.
48. Zhang, S., J. Ma, L. Sheng, D. Zhang, X. Chen, J. Yang, and D. Wang. 2017. Total coumarins from Hydrangea paniculata show renal protective effects in lipopolysaccharide-induced acute kidney injury via anti-inflammatory and antioxidant activities. *Frontiers in Pharmacology* 8: 872.
49. Zhao, S., G. Yang, P.N. Liu, Y.Y. Deng, Z. Zhao, T. Sun, X.Z. Zhuo, J.H. Liu, Y. Tian, J. Zhou, Z. Yuan, and Y. Wu. 2015. miR-590-3p is a novel microRNA in myocarditis by targeting nuclear factor kappa-B in vivo. *Cardiology* 132: 182–188.
50. Zhou, L., and Y. Liu. 2015. Wnt/beta-catenin signalling and podocyte dysfunction in proteinuric kidney disease. *Nature Reviews. Nephrology* 11: 535–545.
51. Zu, C., S. Liu, W. Cao, Z. Liu, H. Qiang, Y. Li, C. Cheng, L. Ji, J. Li, and J. Li. 2017. MiR-590-3p suppresses epithelial-mesenchymal transition in intrahepatic cholangiocarcinoma by inhibiting SIP1 expression. *Oncotarget* 8: 34698–34708.